

Supporting information

DVB-cross-link latex microspheres to uniformly host Eu(III) chelates with moderate swelling capacity for high performance quantitative LFIA strips

Jiannan Jia^{a,b,d}, Hongjian Chen^a, Songle Wang^a, Yunpeng Wang^a, Qike Wang^a, Dong Chen^f, Shisheng Ling^f, Zhenzhen Ge^f, Wenkun Dong^f, Mi Yan^{a,c}, Zhiyu Wang^a, Xianping Fan^a, Xu Liang^e, Qiang Xu^{b,*} and Xvsheng Qiao^{a,c,*}

^a *School of Material Science and Engineering, Zhejiang University, Hangzhou 310058, China*

^b *Ocean Academy, Zhejiang University, Zhoushan 316021, China*

^c *State Key Laboratory of Baiyunobo Rare Earth Resource Researches and Comprehensive Utilization, Baotou Research Institution of Rare Earths, Baotou 014030, China*

^d *Interdisciplinary Student Training Platform for Marine areas, Zhejiang University, Hangzhou 310027, China*

^e *Ocean College, Zhejiang University, Zhoushan 316021, China*

^f *Assure Tec. (Hangzhou) Co.,Ltd, Hangzhou 310015, China*

*Corresponding authors: qiaoxus@zju.edu.cn (X.Qiao)

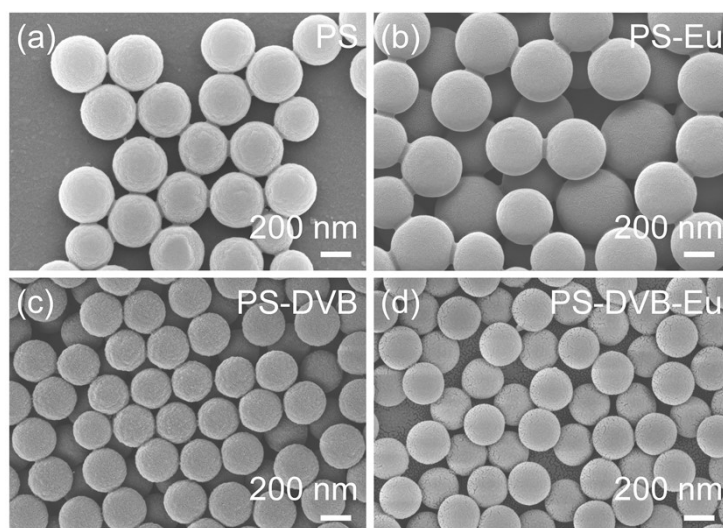


Figure S1 SEM images of (a) PS, (c) PS-DVB microspheres, and (b) PS-Eu, (d) PS-DVB-Eu fluorescent microspheres.

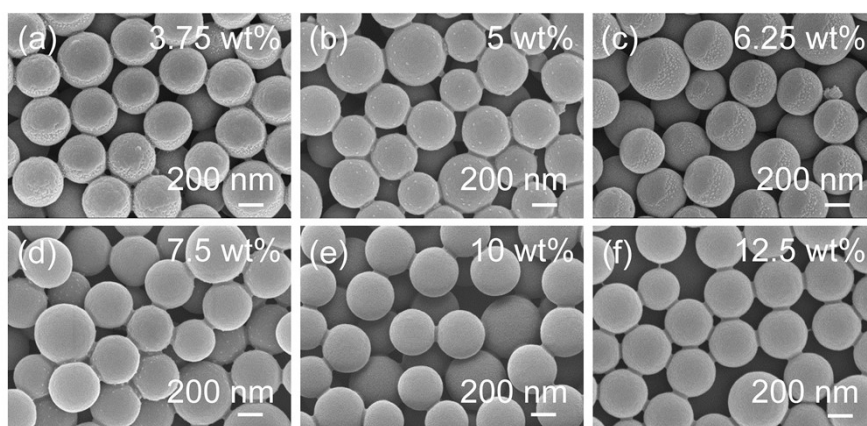


Figure S2 SEM images of fluorescent microspheres prepared with different amount of $\text{Eu}(\text{TTA})_3(\text{TPPO})_2$: (a) 3.75 wt%; (b) 5.00 wt%; (c) 6.25 wt%; (d) 7.50 wt%; (e) 10.0 wt%; (f) 12.5 wt%. (wt% refers to the mass percentage of PS)

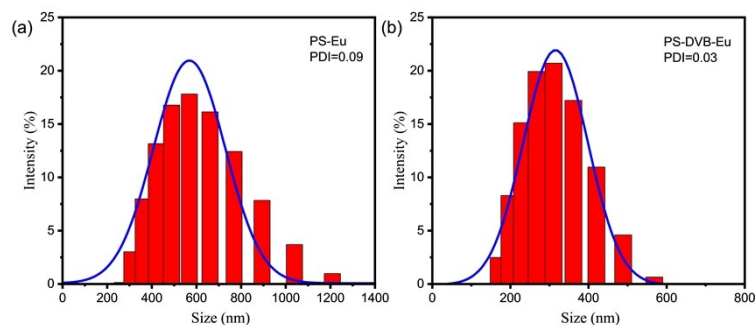


Figure S3 The distribution of particle size and PDI value of (a) PS-Eu and (b) PS-DVB-Eu fluorescent microspheres.

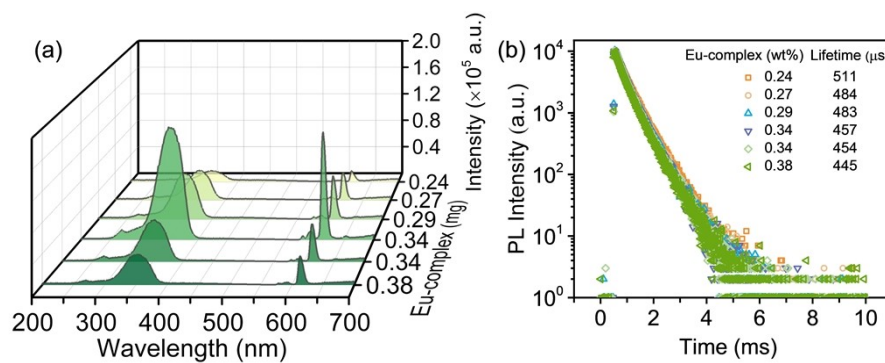


Figure S4 (a) Fluorescence excitation and emission spectra and (b) fluorescence decay curves of PS-Eu fluorescent microspheres with different equivalent concentration of Eu-complex.

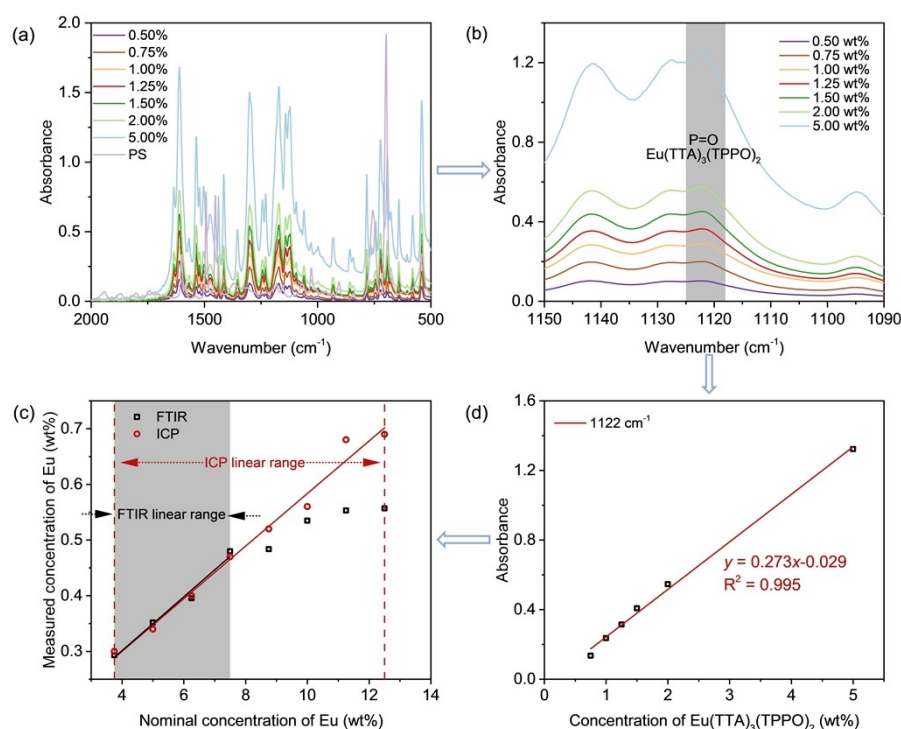


Figure S5 (a) FTIR spectra of standard $\text{Eu}(\text{TTA})_3(\text{TPPO})_2$ samples with gradient concentrations; (b) FTIR spectra after subtracting the baseline; (c) measured concentration of Eu from FTIR method and ICP-MS method; (d) $\text{Eu}(\text{TTA})_3(\text{TPPO})_2$ concentration calibration curve at 1122 cm^{-1} .

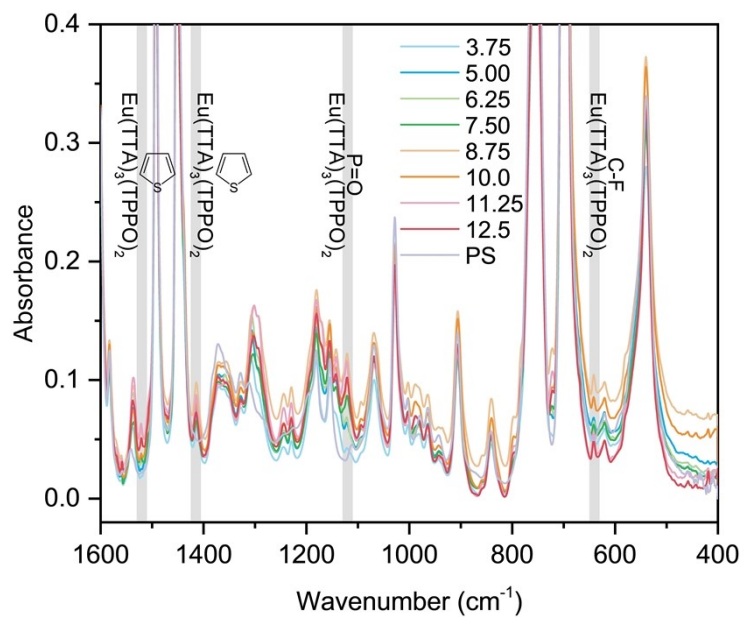


Figure S6 Quantitative FTIR spectra of PS-DVB-Eu fluorescent microspheres with different amount of $\text{Eu}(\text{TTA})_3(\text{TPPO})_2$.

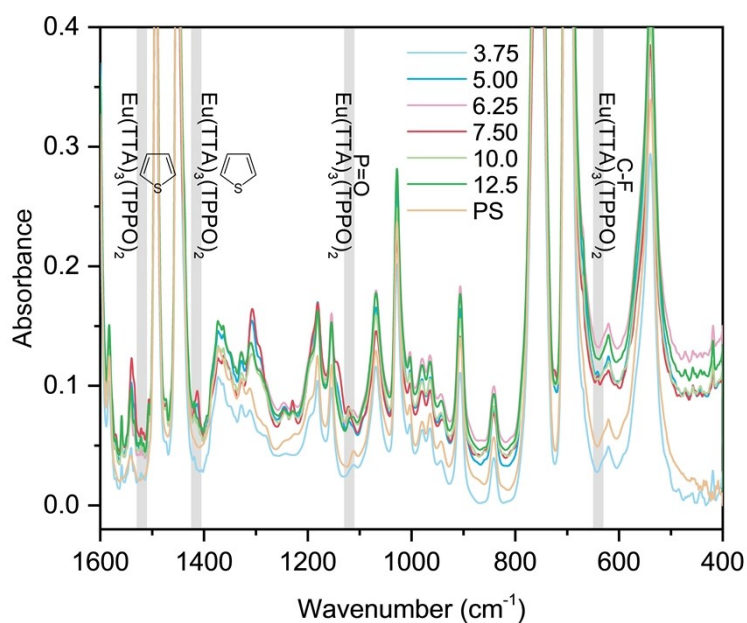


Figure S7 Quantitative FTIR spectra of PS -Eu fluorescent microspheres with different amount of $\text{Eu}(\text{TTA})_3(\text{TPPO})_2$.

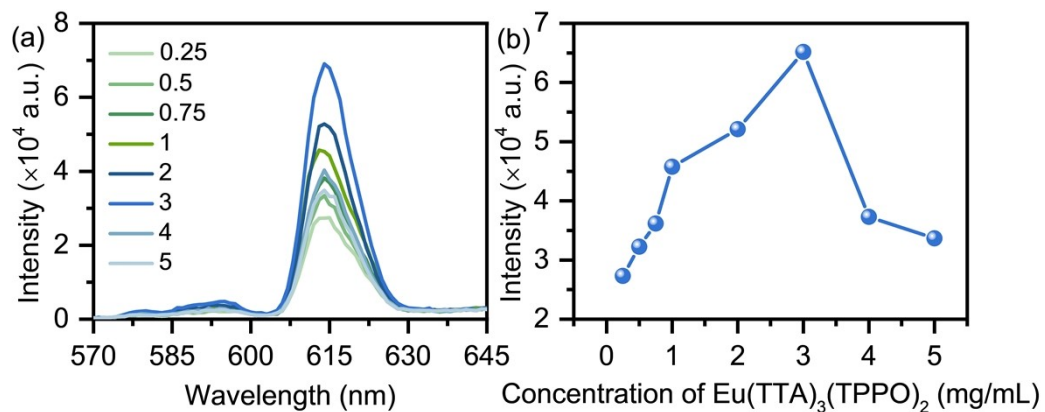


Figure S8 (a) Fluorescence emission spectra and (b) line graph of $\text{Eu}(\text{TTA})_2(\text{TPPO})_3$ complex with different concentration.

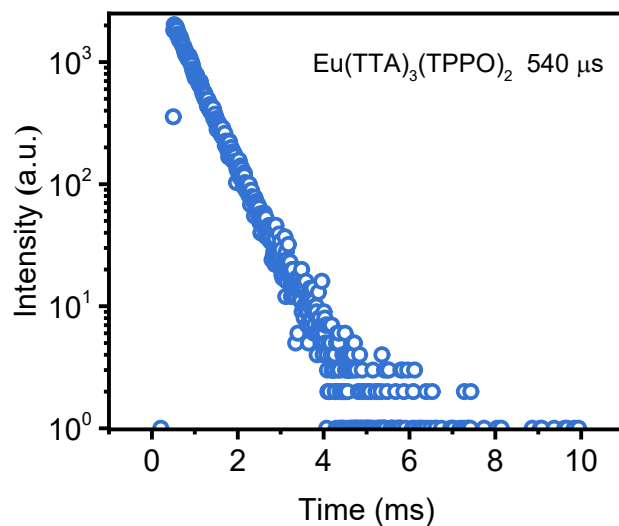


Figure S9 Fluorescence decay curves of $\text{Eu}(\text{TTA})_2(\text{TPPO})_3$ complex.

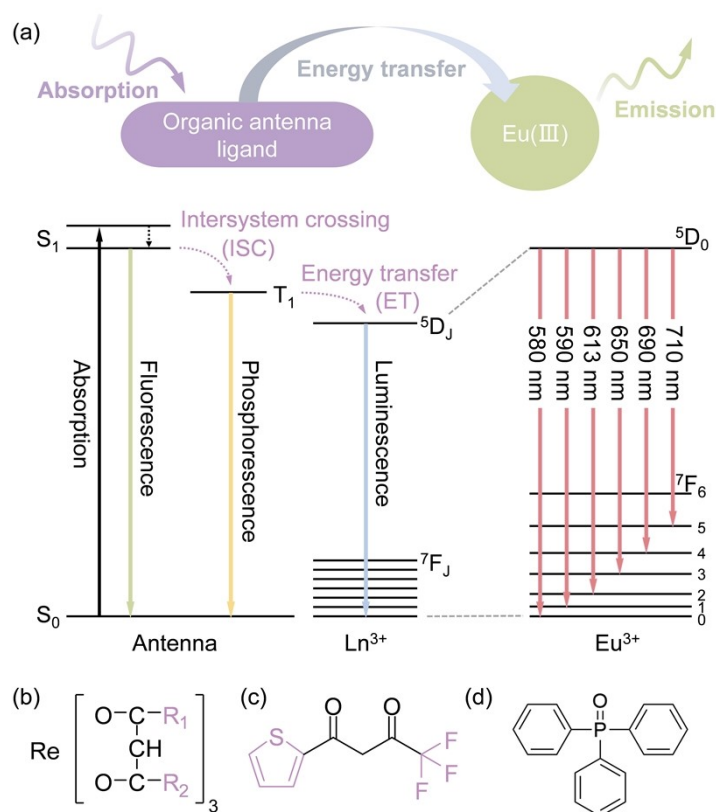


Figure S10 (a) Mechanisms of the antenna effect. S_0 : ground state of the ligand; S_1 : lowest excited singlet state of the ligand; T_1 : excited triplet of the ligand. Chemical structure of (b) β -diketone rare earth complex, (c) TTA and (d) TPPO.

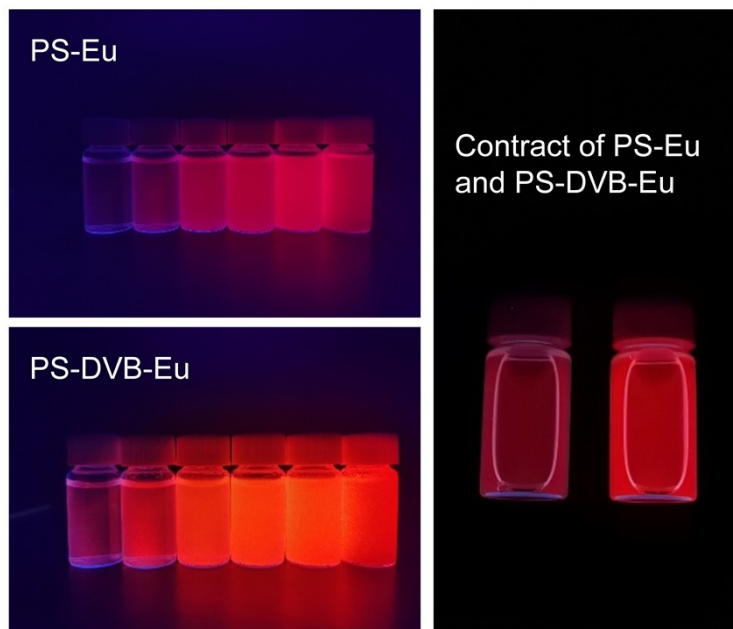


Figure S11 Photograph of PS-Eu and PS-DVB-Eu fluorescent microspheres.

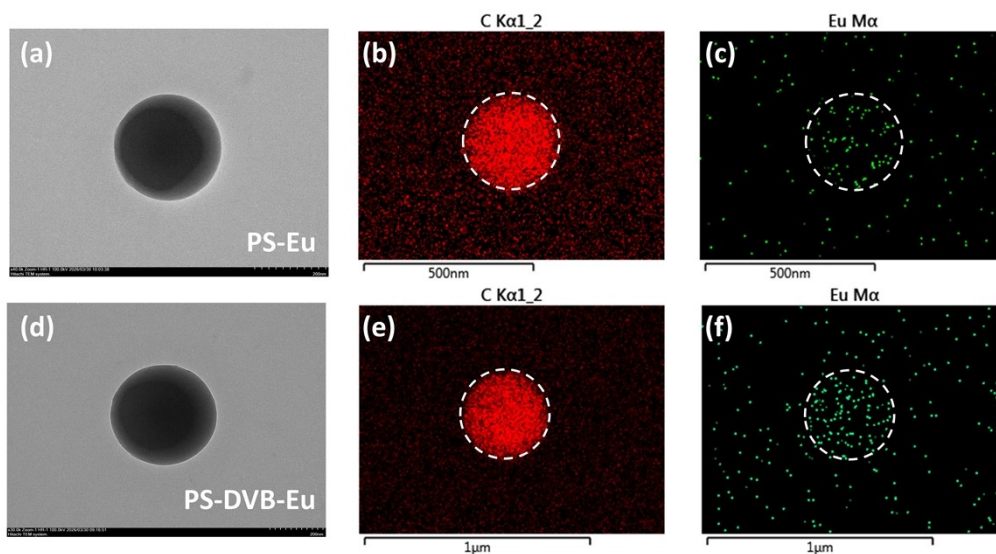


Figure S12 TEM images (a, d) and EDS mapping (b, c, e, f) of PS-Eu and PS-DVB-Eu fluorescent microspheres.

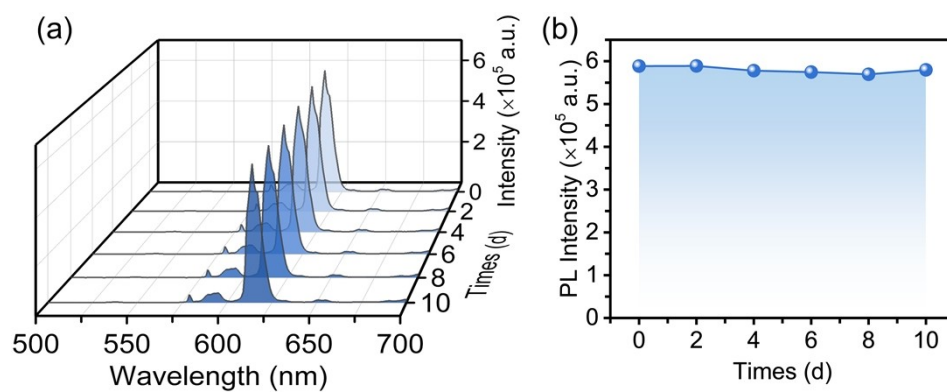


Figure S13 (a) Fluorescent emission spectra and (b) fluorescent stability of PS-DVB-Eu fluorescent microspheres over 10 days.

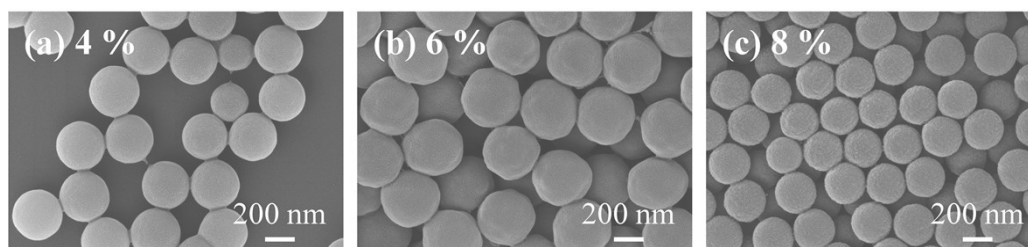


Figure S14 SEM images of PS-DVB microspheres with different concentration of DVB: (a) 4%, (b) 6%, (c) 8%.

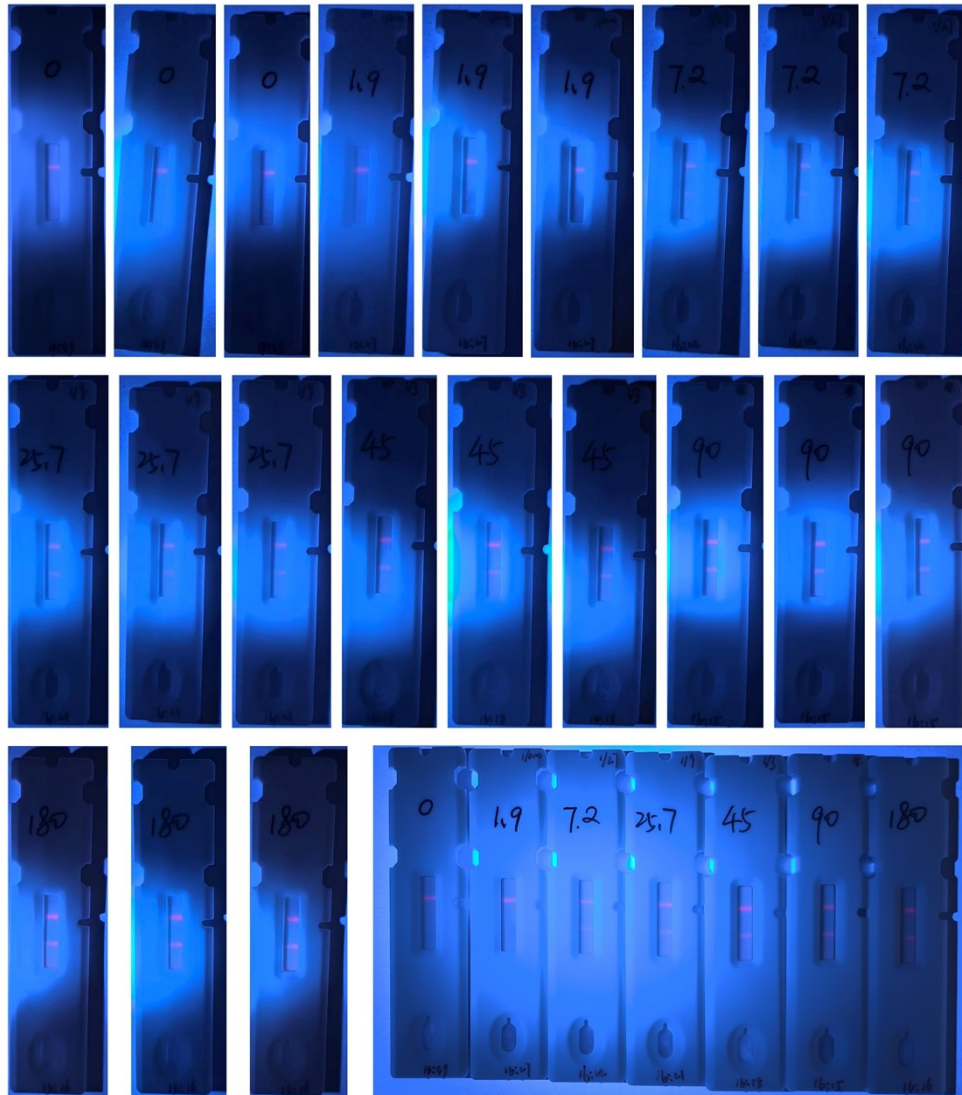


Figure S15 The photograph of LFIA strip for CRP detection using PS-DVB-Eu fluorescent microspheres under UV excitation at 365 nm.

Table S1 Nominal concentration versus equivalent concentration of PS-Eu fluorescent microspheres

Eu-complex	PS -Eu fluorescent microspheres					
Nominal concentration (wt%)	3.75	5.00	6.25	7.50	10.00	12.50
Equivalent concentration (wt%)	0.24	0.27	0.29	0.34	0.34	0.38

Table S2 Zeta potential of PS-Eu and PS-DVB-Eu fluorescent microspheres

samples	Zeta potential (mV)							
PS-Eu	-17.4	-19.32	-13.4	-15.13	-17.98	-13.49		
PS-DVB-Eu	-40.7	-41.37	-48.9	-46.39	-42.15	-49.91	-48.66	-47.98

Table S3 CRP detection using PS-Eu fluorescent microspheres

Concentration (ng/mL)	T1	T2	T3	C1	C2	C3	T/C-1	T/C-2	T/C-3	CV
0	67	0	61	11230	11691	11759	0.006	0	0.0052	-
0.8	587	473	603	9654	10059	10092	0.0608	0.047	0.0598	13.73%
1.9	845	1083	898	8497	10309	8963	0.0994	0.1051	0.1002	3.00%
7.2	5052	5145	6322	10250	10689	11475	0.4929	0.4813	0.5509	7.34%
25.7	13128	14981	13635	10300	11321	11531	1.2746	1.3233	1.1825	5.68%
45	19089	17480	19224	11209	9876	11941	1.703	1.7699	1.6099	4.74%
90	27076	27638	25164	10864	11647	10737	2.4923	2.373	2.3437	3.28%
180	26469	28728	27694	8992	9151	9002	2.9436	3.1393	3.0764	3.27%

Table S4 CRP detection using PS-DVB-Eu fluorescent microspheres

Concentration (ng/mL)	T1	T2	T3	C1	C2	C3	T/C-1	T/C-2	T/C-3	CV
0	3	0	58	12381	11581	12603	0.0002	0	0.0046	-
0.8	292	273	262	9260	9541	10299	0.0315	0.0286	0.0254	10.68%
1.9	471	464	553	8572	10002	10640	0.0549	0.0464	0.052	8.50%
7.2	3142	2892	3183	10684	11496	10690	0.2941	0.2516	0.2978	9.13%
25.7	7145	6727	6477	12013	10189	10063	0.5948	0.6602	0.6436	5.38%
45	10030	11016	10580	9743	11407	11910	1.0295	0.9657	0.8883	7.35%
90	13673	13185	14259	10350	10290	10946	1.3211	1.2813	1.3027	1.53%
180	14399	16137	14523	8810	9684	8591	1.6344	1.6664	1.6905	1.69%